Membrane association of active genes organizes the chloroplast nucleoid structure

V. Miguel Palomar[1, 2], Yoonjin Cho[1], Sho Fujii[1, 3, 4], M. Hafiz Rothi[1], Sarah Jaksich[1], Ji-Hee Min[1], Adriana N. Schlachter[1], Joyful Wang[1], Zhengde Liu[1] and Andrzej T. Wierzbicki[1]

[1]Department of Molecular, Cellular and Developmental Biology, University of Michigan, Ann Arbor, MI 48109, USA

[2]Departamento de Bioquímica, Facultad de Química, Universidad Nacional Autónoma de México, Ciudad de México, 04510, México

[3]Department of Botany, Graduate School of Science, Kyoto University, Kyoto, 606-8502, Japan

[4]Department of Biology, Faculty of Agriculture and Life Science, Hirosaki University, Aomori, 036-8561, Japan

Correspondence: wierzbic@umich.edu

ABSTRACT

DNA is organized into chromatin-like structures that support the maintenance and regulation of genomes. A unique and poorly understood form of DNA organization exists in chloroplasts, which are organelles of endosymbiotic origin responsible for photosynthesis. Chloroplast genomes, together with associated proteins, form membrane-less structures known as nucleoids. The internal arrangement of the nucleoid, molecular mechanisms of DNA organization, and connections between nucleoid structure and gene expression remain mostly unknown. We show that *Arabidopsis thaliana* chloroplast nucleoids have a unique sequence-specific organization driven by DNA binding to the thylakoid membranes. DNA associated with the membranes has high protein occupancy, has reduced DNA accessibility, and is highly transcribed. In contrast, genes with low levels of transcription are further away from the membranes, have lower protein occupancy, and have higher DNA accessibility. Membrane association of active genes relies on the pattern of transcription and proper chloroplast development. We propose a speculative model that transcription organizes the chloroplast nucleoid into a transcriptionally active membrane-associated core and a less active periphery.

SIGNIFICANCE STATEMENT

Long and complex molecules of DNA are precisely organized within cells to support genome maintenance and gene expression. In addition to prokaryotic cells and eukaryotic nuclei, this principle also applies to organelles of endosymbiotic origin, which originated from bacterial ancestors and retain their own genomes. One type of endosymbiotic organelle is the chloroplast, which is present in plant and algal cells and is responsible for photosynthesis. We show that chloroplast DNA is organized by binding to membranes present inside the organelle. We propose that transcription, the initial step in the process of gene expression, plays an important role in organizing the chloroplast nucleoid into a transcriptionally active membrane-associated core and a less active periphery.

INTRODUCTION

Organization of DNA with proteins and RNA is essential for genome maintenance and regulation. In the eukaryotic nucleus, chromatin is a complex multilevel structure, which supports many aspects of genome function. However, canonical eukaryotic chromatin is not the

only form of DNA packaging. Alternative modes of DNA organization are present in mammalian sperm cells [1], dinoflagellates [2], archaea [3], bacteria [4], and viruses [5]. Structural arrangements of DNA in those tissues or organisms rely on distinct protein machineries and provide unique functional impacts.

Mitochondria and plastids originate from bacterial ancestors and contain their own DNA. This DNA is packaged into chromatin-like structures known as nucleoids. Organellar genomes have special properties that have developed over more than a billion years of co-evolution with the eukaryotic cell host. The DNA organization mechanisms of mitochondria and plastids are clearly distinct from what is known in either eukaryotic nuclei or bacteria, making organellar nucleoids an especially unique case of DNA packaging [6,7]. In line with this, nucleoid-associated proteins (NAPs) in the chloroplasts of land plants are atypical. NAPs are thought to help organize DNA and support transcription [8]. However, chloroplasts of land plants do not contain typical bacterial NAPs like HU or IHF. Also, chloroplast NAPs have little in common with nuclear chromatin proteins, and their biochemical functions remain mostly unknown [9]. This indicates that mechanisms of DNA packaging in plastid nucleoids are likely distinct from their bacterial or nuclear counterparts.

The mechanisms of plastid DNA packaging, the internal structure of nucleoids, and their functional impacts remain poorly understood [6]. In most land plants mature chloroplast nucleoids are localized in the stroma, near thylakoid membranes [10,11]. Electron microscopy studies found that the chloroplast nucleoids have a dense and protein-rich central body, which is resistant to high salt treatment and contains 30 to 50% of organellar DNA. The remaining DNA may be observed as protruding fibrils with weaker protein binding [12–14]. The *in vivo* relevance of the central body remains unclear due to the limitations of sample fixation for electron microscopy and insufficient resolution of light microscopy. The function of the central body is also unclear with some evidence favoring this structure as the site of active transcription [11,15] while others suggest that it may be associated with lower levels of transcription [16].

An important property of both bacterial and nuclear DNA organization is the presence of sequence-specific structural features. This means that individual loci have unique patterns of protein binding, DNA accessibility, and subcellular or subnuclear localization to support the unique properties of each locus. In contrast, it is unknown if the chloroplast nucleoid includes a widespread presence of sequence-specific structural features. Some evidence supports the

possibility of the entire genome adopting uniform structural properties [17], while other studies suggest some level of sequence-specificity [18,19]. It remains unknown if chloroplast nucleoids have a sequence-specific pattern of protein binding, DNA accessibility or suborganellar localization. Therefore, it is difficult to predict if transcription, replication, and other processes involving DNA are supported by or control the arrangement of the chloroplast nucleoid.

To determine if the chloroplast nucleoid has a sequence-specific pattern of structural features, we adopted a broad range of genome-wide approaches. We found that the overall protein occupancy on DNA is dominated by transcriptional machinery and has an impact on restricting the accessibility of DNA. The chloroplast genome has a highly complex and sequence-specific pattern of association with plastid membranes. Membrane association is correlated with plastid encoded RNA polymerase (PEP) binding. Moreover, disruption of PEP transcription and/or chloroplast biogenesis leads to alterations of DNA membrane association, which indicates that transcription and chloroplast biogenesis are required for bringing certain genes to the membranes.

RESULTS

Protein binding to chloroplast DNA is dominated by PEP transcriptional machinery

To test if the chloroplast nucleoid has a sequence-specific pattern of protein occupancy on DNA, we performed an *In vivo* Protein Occupancy Display (IPOD) assay [20,21]. This method relies on formaldehyde crosslinking, purification of protein-DNA complexes by phenol extraction, and high throughput sequencing. Stringency of crosslinking has been previously optimized [22]. IPOD performed with purified Arabidopsis chloroplasts revealed a highly complex pattern of protein occupancy on DNA (Fig. 1A), which is consistent with prior low-resolution findings [11,19]. Its most obvious property is strong enrichment on highly transcribed genes, which is reminiscent of the previously reported pattern of Plastid Encoded RNA Polymerase (PEP) binding to DNA [22] (Fig. 1B). This result is also consistent with the known strong representation of RNA polymerase occupancy in bacterial IPOD occupancy traces [21]. Within individual genes, protein occupancy is often enriched on class I promoter regions, which are preferentially bound by PEP [22] (Fig. 1C) but not on class III promoters and class II promoters, which are not bound by PEP (Fig. S1A). Consistently, the IPOD signal and PEP binding to DNA are highly and significantly correlated

on both annotated genes (Fig. 1D) and throughout the entire genome (Fig. S1B). As much as 85% of IPOD variance may be explained by PEP binding (Fig. 1D). This suggests that protein binding to chloroplast DNA is dominated by PEP and potentially other proteins that bind in concert with PEP.

To further test the contribution of PEP to the overall protein occupancy on DNA, we performed IPOD in the *ptac3* mutant. pTAC3, also known as PAP1, is an accessory subunit of PEP and the *ptac3* mutant is expected to lose the majority of PEP transcription [23]. The IPOD signal was reduced almost to the background level in the *ptac3* mutant (Fig. S1CD). This reduction was clear at sequences with the strongest levels of PEP binding [22], including tRNA and rRNA genes (Fig. S1CD). These results further support the predominant contribution of PEP to the overall protein occupancy on DNA.

The presence of a few genomic regions that do not fully follow this relationship between IPOD and PEP binding may be explained by the presence of other nucleoid-associated proteins with weaker or transient binding [8,24–26]. Additionally, more proteins may bind DNA without sequence-specificity, as non sequence-specific interactions may be undetectable by IPOD. Together, these results indicate that there is a complex and sequence-specific pattern of protein binding to DNA in chloroplast nucleoids and that this binding is dominated by PEP transcriptional machinery.

PEP-occupied genes have reduced DNA accessibility

To test if protein occupancy is negatively correlated with DNA accessibility, we adapted the Assay for Transposase-Accessible Chromatin (ATAC-seq), which is a method used to study nuclear genomes and relies on fragmentation of the genome by engineered Tn5 transposomes [27]. In this method, accessible DNA serves as a good substrate for transposon integration, but strong protein binding prevents transposon insertion. We optimized ATAC-seq to study plastid nucleoids and refer to this approach as ptATAC-seq. In our modified protocol, purified chloroplasts are crosslinked with formaldehyde as described previously [22], lysed with a hypotonic buffer, incubated with Tn5 transposomes, and assayed by high throughput sequencing. Purified (naked) DNA that has not been crosslinked is used as a control.

ptATAC-seq on wild type Arabidopsis chloroplasts revealed a relatively complex pattern of Tn5 insertions into the plastid genome (Fig 2A). Observed effects were low and variation

within the eleven biological replicates of this experiment was high (Fig. S2A), which explains why only subsets of the genome had significant enrichments or depletions of Tn5 integration (Fig. 2A). It also indicates that differences in DNA protection detected by Tn5 throughout the chloroplast genome are likely much smaller than in the nuclear genome. To test if low levels of Tn5 integration correspond to high PEP binding and overall protein occupancy, we split genomic bins into groups with significant enrichment of Tn5 integration (accessible), significant depletion of Tn5 integration (protected) or no significant change (undetermined) (Fig. 2B). Genomic bins marked as accessible had low levels of PEP binding detected by RpoB ptChIP-seq, while bins marked as protected had high levels of PEP binding (Fig. 2C). This indicates that high levels of PEP binding are associated with depletion in Tn5 integration. This may be interpreted as evidence of at least partial DNA protection by PEP and associated proteins, leading to reduced DNA accessibility.

Chloroplast nucleoid is organized by association with the membranes

An important property of chloroplast nucleoids is their association with the thylakoid membranes [10,11]. DNA interactions with the membranes may involve a subset of genes in a sequence-specific pattern. This has been suggested by studies in spinach [18,28]. Interestingly, other studies suggest that DNA association with the membranes may have limited or no sequence specificity [17]. To distinguish between these alternative scenarios, we developed an assay to study sequence-specific DNA-membrane associations on the genome-wide scale (Fig. 3A). The Soluble-Insoluble Nucleoid Fractionation Assay (SOLINA) is based on a well-established approach to separate thylakoid membranes and stroma by centrifugation of lysed chloroplasts [29–34]. In the SOLINA assay, purified Arabidopsis chloroplasts are crosslinked with formaldehyde and lysed using a hypotonic buffer, then DNA is fragmented by partial digestion with Micrococcal nuclease (MNase). Subsequently, the sample is fractionated by centrifugation. The insoluble fraction (pellet) is expected to contain the membranes together with crosslinked DNA. The soluble fraction (supernatant) is expected to contain stroma and DNA fragments, that were not crosslinked to the membranes. DNA is then purified, sonicated to reduce fragment lengths (Fig. S3A), and assayed by high throughput sequencing. The ratio of pellet to supernatant signals is interpreted as enrichment of a particular sequence in the membranes (Fig. 3A).

To test the specificity of the SOLINA assay, we performed western blots with antibodies against membrane- and stroma-localized proteins. RbcL, the stroma-localized large subunit of Rubisco, was detectable only in the soluble fraction (Fig. 3B). In contrast, LHCB1, the membrane-localized subunit of the light-harvesting complex II, was detectable only in the insoluble fraction (Fig. 3B). This is consistent with previous observations [33] and confirms that our approach separates membrane and stromal fractions. To further confirm the specificity of SOLINA, we used the results of a prior study, which identified the region around 16S and 23S rRNA genes as membrane-bound [28]. The outcome of SOLINA-seq was highly consistent with this observation (Fig. 3C), which further supports the specificity of our assay. While we cannot entirely exclude the possibility that properties other than membrane binding may affect DNA fractionation, we interpret the enrichment in insoluble fraction as evidence of membrane association.

Chloroplast DNA showed a complex sequence-specific pattern of membrane association in SOLINA (Fig. 3C). In addition to rRNA genes in the inverted repeats (IR), several other genomic regions in both the large single copy (LSC) and small single copy (SSC) were preferentially associated with the membranes (Fig. 3C). This indicates that preferential membrane association involves a subset of genes in a sequence-specific pattern. This suggests that the chloroplast nucleoid is organized by anchoring DNA to the membranes.

Membrane association is correlated with PEP transcription

Preferential membrane association of rRNA genes and other genomic regions that contain highly transcribed genes (Fig. 3C) suggests that membrane association may be correlated with transcription. To test this hypothesis on the genome-wide scale, we compared membrane association determined by SOLINA with PEP binding to DNA determined by ptChIP-seq. Membrane association and PEP binding were strongly and significantly correlated on annotated genes (Fig. 4A) and throughout the entire plastid genome (Fig. S4A). Consistently, the strongest membrane association was observed on rRNA and tRNA genes (Fig. 4A) and was enriched on class I gene promoters (Fig. S4B), where PEP binding is also enriched [22].

To further validate the observed correlation between PEP binding and membrane association, we asked if the correlation persists in plants grown under different physiological conditions. Prolonged dark treatment is expected to result in a substantial change in the pattern of

chloroplast gene expression [33]. RpoB ptChIP-seq confirmed that 24-hour dark treatment leads to a genome-wide change in the pattern of PEP binding to DNA (Fig. 4B, Fig. S4C). Similarly, the pattern of DNA membrane association detected by SOLINA was also changed upon 24-hour dark treatment (Fig. 4C). Interestingly, the change in PEP binding to DNA was significantly correlated with the change in membrane association (Fig. 4D, Fig. S4D). This further confirms that membrane association is correlated with PEP binding to DNA.

Together, these results suggest that PEP-transcribed regions of the chloroplast genome are preferentially associated with the membranes. In contrast, non-transcribed sequences are not efficiently crosslinked to the membranes due to physical distance and/or lack of crosslinkable protein-DNA interactions.

Disruption of chloroplast development may reduce the overall level of PEP transcription

The observed correlation between PEP binding to DNA and membrane association does not imply causality. To test if disruption of chloroplast development has an impact on the pattern of transcription, we used two mutants, which disrupt chloroplast biogenesis. Magnesium protoporphyrin IX methyltransferase (CHLM) is required for chlorophyll biosynthesis and the *chlm* mutants have disrupted thylakoid formation and yellow phenotypes [35,36] (Fig. S5A). Similar phenotypes are observed in the *chl27* (*chl27-t*) mutant (Fig. S5A), which knocks down a subunit of the magnesium protoporphyrin IX monomethyl ester cyclase, another enzyme involved in chlorophyll biosynthesis [37].

To test the impact of chloroplast development on the pattern of transcription, we performed RpoB ptChIP-seq in *chlm* and *chl27* mutants. The *chlm* mutant showed no detectable impact on the pattern of PEP binding to DNA (Fig. 5B, Fig. S5B). This suggests that disruptions of chloroplast development caused by CHLM deficiency are not sufficient to change the pattern of transcription. Interestingly, the *chl27* mutant showed a moderate but significant reduction in the levels of PEP binding to DNA (Fig. 5A). This reduction was observed throughout all PEP-transcribed genes and was highly uniform (Fig. 5C) in contrast to strong locus-specific effects observed in the *sig2* mutant [22] (Fig. 5D, Fig. S5B). This indicates that CHL27 deficiency leads to the overall reduction of PEP transcriptional activity with no detectable locus-specific effects. Consistently, the accumulation of PEP subunits RpoB and RpoC1 was not reduced in *chlm* and *chl27* (Fig. 5E).

These results indicate that disruption of chloroplast development caused by attenuated chlorophyll biosynthesis may have an indirect impact on the overall PEP activity, but have minimal influence on the sequence-specific pattern of PEP binding.

PEP transcription impacts DNA membrane association

The indirect impact of chloroplast biogenesis on the overall level of PEP binding does not eliminate the possibility that the pattern of transcription may affect DNA membrane association. To test this hypothesis, we used mutants defective in sigma factors SIG2 and SIG6, which are known to directly recruit PEP to specific genes [38–40] and affect genome-wide patterns of PEP binding to DNA [22]. SOLINA performed with *sig2* and *sig6* mutants revealed broad disruptions of DNA membrane association (Fig. 6A, Fig. S6AB). Comparison of SOLINA to previously published RpoB ptChIP-seq in *sig2* [22] demonstrated a significant correlation between changes in PEP binding to DNA and changes in DNA association with the membranes (Fig. 6B). An even stronger correlation was observed in *sig6* (Fig. 6C), which has a more pronounced impact on PEP binding to DNA than *sig2* [22]. This indicates that reduction of PEP binding to specific genes in sigma factor mutants leads to a reduction in membrane association at those genes.

To test if *sig2* and *sig6* may affect membrane binding indirectly by disrupting the thylakoid membranes, we assayed the accumulation of plastid membrane lipids monogalactosyldiacylglycerol (MGDG) and digalactosyldiacylglycerol (DGDG). While the level of DGDG was unchanged, MGDG content was decreased to ~60 % in these mutants (Fig. S6C), consistent with previous studies showing decreases of internal membrane structures in plastids of *sig2* and *sig6*, in comparison with the wild type [39,40]. Furthermore, the decreases of chlorophyll accumulation in *sig2* and *sig6* mutants were similar to that in *chlm* and *chl27* mutants (Fig S6D). These results demonstrate that the thylakoid formation was partially impaired in *sig2* and *sig6* mutants and suggest that *sig2* and *sig6* mutants may impact DNA membrane association by a combination of direct and indirect mechanisms, which is consistent with the proposed presence of both direct and indirect impacts of *sig2* and *sig6* on chloroplast transcription [22].

Together, these results indicate that transcription affects DNA membrane association directly by affecting DNA binding of individual genes and/or indirectly by affecting the thylakoid formation probably due to the loss of photosynthetic proteins in the membranes.

Disruption of chloroplast development impacts DNA membrane association

The proposed presence of indirect effects of *sig2* and *sig6* on DNA membrane association predicts that *chlm* and *chl27* mutants should also disrupt DNA membrane association. To test this prediction, we performed SOLINA in *chlm* and *chl27*. Both mutants significantly affected DNA membrane association (Fig. 7A-C). Moreover, in *chl27*, reductions of the SOLINA signal were correlated with the reductions of PEP binding (Fig. 7D). These results indicate that chloroplast development has an impact on DNA membrane association.

Chloroplast development and thylakoid membrane formation may be the sole mechanism affecting DNA membrane association. Alternatively, both thylakoid formation and PEP transcription may contribute to DNA membrane binding. To distinguish between these possibilities, we directly compared SOLINA results from the *chlm* mutant, which partially disrupts chloroplast development and thylakoid formation [35,36] but has no impact on PEP binding to DNA (Fig. 5B) with results from *chl27*, which partially disrupts chloroplast development and thylakoid formation [37] but also has an impact on the overall PEP binding to DNA (Fig. 5C). *chl27* had a substantially greater impact on membrane association than *chlm*, especially on rRNA and tRNA genes (Fig. 7E, Fig. S7A). Although differences between those mutants should be interpreted carefully, our results indicate that not only thylakoid membrane integrity but also PEP transcription contributes to associating actively transcribed genes with the membranes.

DISCUSSION

We propose a model of chloroplast nucleoid organization where DNA is organized in a sequence-specific manner and the main determinants of this specificity include the level of transcription and thylakoid membrane formation. In this model, highly transcribed genes like *psbA*, *rbcL*, many tRNA genes, and ribosomal RNA genes are preferentially attached to the thylakoid membranes. Membrane-associated DNA has high levels of overall protein occupancy, which is dominated by PEP and related proteins. Other proteins may also bind to membrane-associated DNA, but this binding is either less prominent, weaker, less sequence-specific, or less susceptible to formaldehyde crosslinking. High protein binding instigates a certain level of DNA protection, likely caused by the widespread presence of PEP and proteins, which bind in concert with PEP. Recruitment of active genes to the membranes requires both PEP transcription and the presence of intact thylakoid membranes.

Regions of the genome with low levels of transcription are depleted in binding to the membranes. This may be caused by their presence in the stroma or by less efficient formaldehyde crosslinking to membrane proteins. DNA with low levels of transcription has low protein occupancy and no detectable DNA protection, which may be caused by an overall low amount or low sequence-specificity of protein binding or limited formaldehyde crosslinking of bound proteins. It should be noted that we have no reasons to expect that peripheral location of DNA is incompatible with PEP transcription. It remains possible that DNA molecules or regions without strong membrane binding may still serve as templates for PEP.

Highly transcribed and membrane-associated DNA in our model likely corresponds to the biochemically detected Transcriptionally Active Chromosome and the central body observed using EM [11,15]. Untranscribed and unprotected DNA that is not associated with the membranes is consistent with the DNA fibrils observed in EM [11,15]. It should, however, be noted that there may be only limited equivalency of structures detected using different approaches.

Our model is based on the interpretation that the insoluble chloroplast fraction corresponds to the membranes and membrane-bound factors. This interpretation has strong support in the literature [29–34], protein composition of soluble and insoluble fractions, and consistency of SOLINA results with published data. It remains possible that properties other than direct binding to the membranes may drive certain molecules to the pellet during chloroplast fractionation, which is a potential limitation of our interpretation.

Membrane association of active genes relies on both the pattern of PEP transcription and chloroplast development, including the presence of proper thylakoid membranes. These two processes are very difficult to tease apart because PEP transcription is required for chloroplast development (as observed in *sig2* and *sig6* mutants) [39,40] and chloroplast development may impact transcription (as observed in the *chl27* mutant and some thylakoid lipid-deficient mutants [41,42]). It remains possible that chloroplast development and establishment of proper thylakoid membranes may be the sole determinant of DNA-membrane association and the impact of PEP transcription may be mostly indirect. However, we find this scenario unlikely. Instead, our results indicate that both PEP transcription and chloroplast development contribute to establishing the sequence-specific pattern of DNA-membrane association. This is supported by coordinated changes in PEP binding and DNA membrane association in darkness when the chloroplast ultrastructure does not largely change. It is also supported by the observation that

chl27, which impacts both chloroplast development and PEP transcription, has a greater impact on DNA membrane association than *chlm*, which impacts chloroplast development but not PEP transcription. The influence of other processes like NEP transcription, replication, or DNA repair on membrane binding remains unknown. It is also unknown how the presence of multiple copies of the genome in each chloroplast [43] contributes to the chloroplast genome organization.

The impact of membrane binding on transcription, gene regulation and proper plastid function remains unknown. Large differences of PEP-DNA binding and SOLINA enrichment between the light phase and dark phase indicate that the pattern of membrane binding is dynamically rearranged when the levels of transcription change in response to changing environmental conditions. While our experiments using sigma factor mutants place transcription upstream of membrane binding, a reciprocal relationship is possible. Membrane association may have an impact on establishing the proper pattern of gene expression, chloroplast biogenesis and response to the environment.

Mechanisms that recruit transcribed DNA to the membranes remain unknown. One possibility is association of PEP with the membranes [33], although core and peripheral subunits of PEP are soluble [44] and such association would likely have to be indirect. Additionally, certain nucleoid-associated proteins like MFP1, PEND, TCP34 and pTAC16 are expected to directly bind to the membranes [45–48]. If they also preferentially bind to transcribed DNA, they could contribute to DNA recruitment to the membranes. Another explanation is possible for genes encoding membrane proteins, including subunits of photosynthetic complexes. Ribosomes translating such proteins have been shown to attach to the thylakoid membranes [34]. Assuming at least some co-transcriptional translation, DNA could be tethered to the membranes by coupled transcription-translation-membrane insertion, also known as transertion [49,50]. In this scenario, membrane binding could facilitate efficient gene expression. One additional speculative explanation of membrane binding of active genes is formation of membrane surface biomolecular condensates including PEP [51], which could provide a local environment supporting transcription. Resolving the mechanism of membrane recruitment remains an important goal for future studies.

EXPERIMENTAL PROCEDURES

Plant materials and growth conditions

We used *Arabidopsis thaliana* wild-type Columbia-0 (Col-0) ecotype plants for all the experiments in this work, and we included the following genotypes: *ptac3* (SALK_110045) [23], *sig2-2* (SALK_045706) [52], *sig6-1* (SAIL_893_C09) [39], *chlm* (SALK_110265) [35] and *chl27-t* (SALK_009052) [37]. Seeds were stratified in darkness at 4ºC for 48 hours and grown on soil at 22ºC under white LED light (100 μmol m^{-2} s^{-1}) in 16h/8h day/night cycle for 14 days, or grown on 0.5X MS plates (0.215% MS salts, 0.05% MES-KOH, 1% sucrose, pH 5.7, 0.65% agar) for 4 days at 22ºC under constant white LED light (50 μmol m^{-2} s^{-1}). For experiments requiring extended dark treatment, 14 days-old plants were exposed to 24-hour darkness treatment. Subsequent chloroplast isolation and cross-linking were performed avoiding light exposition. Control samples were collected after 3 hours of light exposition.

Chloroplast enrichment and crosslinking

Chloroplasts from 14-day-old seedlings were enriched and crosslinked following the protocol adapted by [22] based on the original protocol from [53]. Chloroplasts were quantified by the amount of chlorophyll [54] and the amount of chloroplasts corresponding to 100 μg chlorophyll was used, unless indicated otherwise. In experiments using seedlings, 50 4 days-old seedlings were crosslinked in a solution of 4 % formaldehyde with vacuum treatment for 10 minutes followed by ice incubation for 4 hours. Formaldehyde was quenched by adding glycine to reach a concentration of 600 mM and vacuum treated for 5 minutes, solution of formaldehyde and glycine was discarded. Cross-linked seedlings were homogenized in the Chloroplast enrichment buffer (0.33 M sorbitol, 30 mM HEPES-KOH [pH 7.5], 0.001% β-mercaptoethanol) using a microtube pestle, and filtered through 2 layers of miracloth by centrifuging for 5 minutes at 1500 g. The pellet composed of an enriched chloroplast fraction was resuspended in the appropriate buffer for downstream experiments.

Chloroplast IPOD

Protein occupancy in the chloroplast nucleoid was assayed by adapting the previously described IPOD technique [20,21]. Crosslinked enriched chloroplasts were solubilized in 1X MNase reaction buffer (50 mM Tris-HCl pH 8.0, 5 mM $CaCl_2$)] supplemented with 100 μg of RNase A and incubated for 20 minutes on ice; MNase was added to obtain fragments ranging from 100 to 200

bp and the sample was incubated for 10 minutes at 30 ˚C. MNase reaction was stopped by adding EDTA to a final concentration of 100 mM and a fraction was used as the input control. The stopped reaction was combined with 1 volume of 100 mM Tris base and 1 µl of 10 % BSA. One volume of 25:24:1 phenol:chloroform:isoamyl alcohol was added to the sample, vortexed for 10 seconds, incubated for 10 minutes at room temperature, mixed again, and centrifuged at 21,130 g for 2 minutes at room temperature. The aqueous and organic phases were taken out and discarded by carefully bringing the interphase protein disk against the tube wall. The disk was resuspended by the addition of 1 volume TE buffer (10 mM Tris pH 8.0, 1 mM EDTA pH 8.0) and 1 volume Tris base, and extracted using 1 volume of 24:1 chloroform:isoamyl alcohol, mixed and centrifuged as before. The disk was resuspended in 1 volume of TE buffer and further isolated with 1 volume 24:1 chloroform:isoamyl as described. The final protein disk was solubilized in ChIP elution buffer (100 mM Tris-HCl pH 8.0, 10 mM EDTA, 1 % SDS) and subjected to reverse cross-linking and DNA isolation as reported by [22,55].

ptChIP-seq

ptChIP-seq experiments to detect RpoB binding to DNA were performed as described previosuly [22].

ptATAC-seq

DNA accessibility in the chloroplast nucleoid was assessed with Tn5 transposition by adapting a previously described nuclear ATAC-seq protocol [27]. Crosslinked enriched chloroplasts from 14-day old plants corresponding to 1 µg chlorophyll were resuspended in 1X Tn5 reaction buffer (Illumina) and assayed according to the manufacturer's instructions, except using 0.1 amount of Tn5 to avoid overtagmentation. For naked DNA controls, 50 ng of DNA purified from non-crosslinked chloroplast was used side by side with chloroplast samples. The tagmented DNA was purified using the MinElute PCR purification kit following the manufacturer's instructions. High throughput sequencing libraries were generated as reported [27].

SOLINA

Membrane and stromal-enriched DNA regions were identified by the Soluble-Insoluble Nucleoid Fractionation Assay (SOLINA). Crosslinked enriched chloroplasts were resuspended in 1X

MNase reaction buffer (50 mM Tris-HCl pH 8.0, 5 mM $CaCl_2$) and incubated on ice for 20 minutes to burst chloroplasts. The ice incubation step was skipped for SOLINA involving *chl27* and *chlm* mutants. MNase was added at a range of concentrations to obtain fragment lengths between 100 and 300 bp in the soluble fraction and incubated at 30ºC for 10 minutes. MNase reaction was stopped by adding EDTA and EGTA at a final concentration of 10 mM each, and the sample was centrifuged at 21,130 g for 10 minutes at 4ºC. The soluble fraction was transferred to a new tube, and the pellet was resuspended in 1 volume of ChIP elution buffer. SDS was added to the soluble fraction to reach a final concentration of 1%. Reverse crosslinking and DNA isolation for both fractions was performed as described [22,55]. Purified DNA was sonicated as described [22] to obtain similar length distributions between pellet and supernatant fractions.

Immunoblot analysis

Proteins from SOLINA assays were extracted by resuspending samples in protein extraction buffer (20 mM Tris-HCl (pH 6.8), 3% β-mercaptoethanol, 2.5% SDS, 10% sucrose) and incubated for 1.5 h at room temperature. 20 μg of proteins from the pellet fraction and its equivalent volume of the supernatant fraction were separated by SDS-PAGE. To detect RbcL, polyclonal anti-RbcL antibody (PhytoAB catalog number PHY0096A) and anti-rabbit IgG antibody conjugated with horseradish peroxidase (Thermo catalog number PI314) were used as the primary and secondary antibodies, respectively. For LHCB1 detection, we used the polyclonal anti-LHCB1 antibody from Agrisera (catalog number AS01 004) and the same secondary antibody; both detections were made at the same time by splitting the membranes in half considering the apparent protein molecular weights. Protein bands were visualized using chemiluminescence reagents (ECL Prime Western Blotting Detection Reagent, Amersham) and an ImageQuant LAS 4000 imager or blue films (Kodak).

To detect RpoB, RpoC1, and Actin in Col-0 wild type, *chl27*, and *chlm* mutants, total proteins were extracted by 2x SDS loading buffer (125 mM Tris-HCl, pH 6.8, 2% SDS, 0.05% Bromophenol blue, 20% glycerol, 200 mM β-Mercaptoethanol). Anti-RpoB antibody (PhytoAB catalog number PHY 1239), anti-RpoC1 antibody (PhytoAB catalog number PHY 0381A), anti-Actin antibody (Agrisera catalog number AS13 2640), and anti-rabbit IgG antibody conjugated with horseradish peroxidase (Thermo catalog number PI314) were used. Protein bands were

visualized using chemiluminescence reagents (ECL Prime Western Blotting Detection Reagent, Amersham) and an ImageQuant LAS 4000 imager or blue films (Kodak).

Chlorophyll level determination

Chlorophylls were extracted by immersing seedlings in 80% acetone at 4ºC in darkness for 2 or 3 days. To determine chlorophyll concentration, the absorbance at 663.5 and 646.5 nm was measured with a UVmini 1240 spectrophotometer (Shimazu) as reported [56].

Lipid analysis

Total lipids extracted from seedlings were separated by thin-layer chromatography with developing solvent of acetone:toluene:water (136:46:12) as reported [57]. MGDG, DGDG, and other membrane lipids visualized with 0.01% primuline in 80% acetone were isolated and methyl esterified by incubating with 1 M HCl in methanol at 85 ºC for 1.5 h. Fatty acid methyl esters were quantified by CG-17A gas chromatography (Shimazu) with pentadecanoic acid methyl ester as an internal standard.

Data analysis

For chloroplast IPOD, ptChIP-seq, ptATAC-seq, and SOLINA, we performed mapping to the chloroplast reference genome as described previously [22]. Briefly, obtained raw sequencing reads were trimmed using trim_galore v.0.6.7 (https://www.bioinformatics.babraham.ac.uk/projects/trim_galore/) with cutadapt v.3.5 [58] and mapped to the TAIR10 Arabidopsis plastid genome (www.arabidopsis.org) using Bowtie2 v.2.4.4 [59]. Read counts on defined genomic regions (annotated genes or bins) were determined using samtools v.1.13 [60] and bedtools v.2.30.0 [61]. For ptATAC-seq Tn5 insertions were counted in 250 bins spanning the entire chloroplast genome. Protection was calculated as ratio of the number of insertions in the crosslinked nucleoid sample to the number of insertions in the uncrosslinked naked DNA control. Significance of differences between chloroplast nucleoid and naked DNA control in 11 biological replicates of each was established using the negative binomial model implemented in the NBPseq package [62]. For IPOD, data was calculated as ratio of reads-per million (RPM)-normalized read counts of IPOD to input samples. In case of ptChIP-seq data, ChIP signal was calculated as ratio of RPM-normalized ChIP to input. ChIP enrichment

was calculated by dividing ChIP signal of each gene or bin by the median ChIP signal of genes within the *rpoB* operon [22]. In SOLINA, signal is calculated by dividing RPM-normalized read counts in the pellet fraction by supernatant fraction.

ACCESSION NUMBERS

The sequencing data from this study have been submitted to the NCBI Gene Expression Omnibus (GEO; http://www.ncbi.nlm.nih.gov/geo/) under accession number GSE228230. Sequencing data presented in this study are available through a dedicated publicly available Plastid Genome Visualization Tool (Plavisto) at http://plavisto.mcdb.lsa.umich.edu.

ACKNOWLEDGEMENTS

This work was supported by a grant from the National Science Foundation (MCB 1934703) to A.T.W and partially by UNAM-PAPIIT grant IA203424 to V.M.P. S.F. was supported by grants from the Japanese Society for the Promotion of Science (19J01779, 20K15819). We thank Lydia Freddolino for critical reading of the manuscript. We also thank Kosei Noto and Yushi Kurotaki for assisting with lipid analysis.

FIGURE LEGENDS

Figure 1. Protein binding to chloroplast DNA is dominated by PEP transcriptional machinery.

A. Genome-wide pattern of protein occupancy on DNA detected by IPOD. Signal from IPOD in Col-0 wild-type 14 days old plants was calculated in 50-bp genomic bins and plotted throughout the entire plastid genome. Genome annotation including genomic regions, positions of annotated genes [22], and names of selected individual genes is provided on top of the plot. Average enrichment from four independent biological replicates is shown. The light blue ribbon indicates standard deviation.
B. Previously published genome-wide pattern of PEP binding to DNA [22]. Signal enrichment from ptChIP-seq using αRpoB antibody in 14 days old Col-0 wild-type plants was calculated in 50-bp genomic bins and plotted throughout the entire plastid genome. Average enrichment and standard deviation from three independent biological replicates are shown.

C. Preferential protein occupancy on PEP gene promoters. IPOD and RpoB ptChIP-seq signal [22] from 14 days old Col-0 wild-type was calculated in 10-bp genomic bins and plotted at *psbA*, *psbE*, *psbB* and *rbcL* loci. Average signal from four (IPOD) or three (ptChIP-seq) independent biological replicates are shown. Ribbons indicate standard deviations. Gray vertical lines indicate positions of the annotated promoters. Genome annotation is shown on top.

D. Protein occupancy and PEP binding are significantly correlated. IPOD signal and RpoB ptChIP-seq signal [22] were compared on annotated genes. Data points are color-coded by function and show averages from three (ptChIP-seq) or four (IPOD) biological replicates. Error bars indicate standard deviations. The blue line represents the linear regression model.

Figure 2. PEP-occupied genes have reduced DNA accessibility.

A. Genome-wide pattern of DNA accessibility detected by ptATAC-seq. Signal from ptATAC-seq in 14 days old Col-0 wild-type plants was calculated and plotted in 250 bins covering the entire plastid genome. Y axis represents ratio of insertions in crosslinked nucleoid to insertions in purified (naked) DNA. Genome annotation including genomic regions, positions of annotated genes [22], and names of selected individual genes is provided on top of the plot. Average signal from eleven independent biological replicates is shown. Red shading indicates significant accessibility and blue shading indicates significant protection identified using a negative binomial model FDR ≤ 0.05. Individual biological replicates are shown in Fig. S2A.

B. Identification of genomic bins with significant accessibility or protection. Negative binomial model (FDR ≤ 0.05) was used to identify genomic bins with significant enrichment (accessible) or depletion (protected) of Tn5 insertions. Regions with no significant change (FDR > 0.05) were identified as undetermined. Individual data points within boxplots are averages from eleven biological replicates.

C. Protected genomic regions have high PEP binding. Previously published RpoB ptChIP-seq signal [22] plotted on genomic bins identified as accessible, protected or undetermined (Fig. 2B). Individual data points within boxplots are averages from three biological replicates.

Figure 3. Chloroplast nucleoid is organized by association with the membranes

A. Workflow of the Soluble-Insoluble Nucleoid Fractionation Assay (SOLINA).
B. Validation of SOLINA by western blot demonstrating presence of RbcL in the soluble (stroma) fraction and LHCB1 in the insoluble (membrane) fraction. Units of MNase and fractions are labeled on the bottom of the panel. S indicates supernatant and P indicates pellet. Star indicates a non-specific band.
C. Genome-wide pattern of membrane association identified by SOLINA. Signal from SOLINA in Col-0 wild-type 4 days old plants was calculated in 50-bp genomic bins and plotted throughout the entire plastid genome. Genome annotation including genomic regions, positions of annotated genes [22], and names of selected individual genes is provided on top of the plot. Average from three independent biological replicates is shown. The light green ribbon indicates standard deviation.

Figure 4. Membrane association is correlated with PEP transcription.

A. Membrane association and PEP binding are significantly correlated. SOLINA signal and RpoB ptChIP-seq signal from 4 days old plants were compared on annotated genes. Data points are color-coded by function and show averages from three biological replicates. Error bars indicate standard deviations. The blue line represents the linear regression model.
B. Extended dark treatment affects the pattern of PEP binding to DNA. RpoB ptChIP-seq was performed using 14 days old Col-0 wild-type plants collected during the day or after extended dark treatment and enrichment was calculated in 50-bp genomic bins and plotted throughout the entire plastid genome. Genome annotation including genomic regions, positions of annotated genes [22], and names of selected individual genes is provided on top of the plot. Average enrichments from three independent biological replicates are shown. Ribbons indicate standard deviations.
C. Extended dark treatment affects the pattern of membrane association. SOLINA was performed on 14 days old Col-0 wild-type plants collected during the day or after extended dark treatment and signal was calculated in 50-bp genomic bins and plotted

throughout the entire plastid genome. Average enrichments from three independent biological replicates are shown. Ribbons indicate standard deviations.

D. Changes in membrane association and PEP binding after extended dark treatment are significantly correlated. Changes in SOLINA signal and RpoB ptChIP-seq signal were compared on annotated genes between plants collected during the day and after extended dark treatment. Data points are color-coded by function and show averages from three biological replicates. Error bars indicate standard deviations. The blue line represents the linear regression model.

Figure 5. Disruption of chloroplast development may reduce the overall level of PEP transcription.

A. Reduction of PEP binding to DNA in the *chl27-t* mutant. RpoB ptChIP-seq enrichment in 4 days old plants was calculated in 50-bp genomic bins and plotted throughout the entire plastid genome. Genome annotation including genomic regions, positions of annotated genes [22], and names of selected individual genes is provided on top of the plot. Average signal from three independent biological replicates is shown. Ribbons indicate standard deviations.

B. The *chlm* mutant has no impact on the pattern of PEP binding to DNA. RpoB ptChIP-seq enrichments in 4 days old Col-0 wild type and the *chlm* mutant were compared on annotated genes. Data points are color-coded by function and show averages from three biological replicates. Error bars indicate standard deviations. The blue line represents the linear regression model. The red line represents no differences.

C. The *chl27-t* mutant had an overall reduction of PEP binding to DNA. RpoB ptChIP-seq enrichments in 4 days old Col-0 wild type and the *chl27-t* mutant were compared on annotated genes. Data points are color-coded by function and show averages from three biological replicates. Error bars indicate standard deviations. The blue line represents the linear regression model. The red line represents no differences.

D. The *sig2* mutant had a combination of overall and locus-specific reductions of PEP binding to DNA. RpoB ptChIP-seq enrichments in 4 days old Col-0 wild type and *sig2* assayed side-by-side with *chlm* and *chl27-t* mutants were compared on annotated genes. Data points are color-coded by function and show averages from three biological

replicates. Error bars indicate standard deviations. The blue line represents the linear regression model. The red line represents no differences.

E. RpoB and RpoC1 are expressed in *chlm* and *chl27-t* mutants. Western blot was performed with whole cell extracts from 4 days old seedlings of Col-0 wild type, *chlm*, and *chl27-t* using anti-RpoB and anti-RpoC1 antibodies. Anti-Actin antibody was used as a loading control.

Figure 6. PEP transcription impacts DNA membrane association.

A. Genome-wide pattern of membrane association in sigma factor mutants. Signal from SOLINA in 4 days old Col-0 wild-type, *sig2* and *sig6* plants was calculated in 1 kb genomic bins distributed throughout the entire plastid genome. Genome annotation including genomic regions, positions of annotated genes [22], and names of selected individual genes is provided on top of the plot. Average signal from three independent biological replicates is shown. Ribbons indicate standard deviations.

B. Changes in membrane association are correlated with changes in PEP binding in the *sig2* mutant. Changes in SOLINA signal and previously published RpoB ptChIP-seq signal [22] between 4 days old Col-0 wild-type and *sig2* mutant were compared on annotated genes. Data points are color-coded by function and show averages from three biological replicates. Error bars indicate standard deviations. The blue line represents the linear regression model.

C. Changes in membrane association are correlated with changes in PEP binding in the *sig6* mutant. Changes in SOLINA signal and previously published RpoB ptChIP-seq signal [22] between 4 days old Col-0 wild-type and *sig6* mutant were compared on annotated genes. Data points are color-coded by function and show averages from three biological replicates. Error bars indicate standard deviations. The blue line represents the linear regression model.

Figure 7. Disruption of chloroplast development impacts DNA-membrane association.

A. Genome-wide pattern of membrane association in chlorophyll biosynthesis mutants, which disrupt chloroplast development and thylakoid membrane structure. Signal from SOLINA in 4 days old Col-0 wild-type, *chlm* and *chl27-t* plants was calculated in 1 kb

genomic bins and plotted throughout the entire plastid genome. Genome annotation including genomic regions, positions of annotated genes [22], and names of selected individual genes is provided on top of the plot. Average signal from four independent biological replicates is shown. Ribbons indicate standard deviations.

B. The *chlm* mutant affects the pattern of DNA membrane association. SOLINA signal in 4 days old Col-0 wild type and the *chlm* mutant were compared on annotated genes. Data points are color-coded by function and show averages from four biological replicates. Error bars indicate standard deviations. The blue line represents the linear regression model. The red line represents no differences.

C. The *chl27-t* mutant affects the pattern of DNA membrane association. SOLINA signal in 4 days old Col-0 wild type and the *chl27-t* mutant were compared on annotated genes. Data points are color-coded by function and show averages from four biological replicates. Error bars indicate standard deviations. The blue line represents the linear regression model. The red line represents no differences.

D. Changes in membrane association are correlated with changes in PEP binding in the *chl27-t* mutant. Changes in SOLINA signal and RpoB ptChIP-seq signal between Col-0 wild-type and *chl27-t* mutant were compared on annotated genes. Data points are color-coded by function and show averages from three or four biological replicates. Error bars indicate standard deviations. The blue line represents the linear regression model.

E. Membrane association of annotated genes is reduced in the *chlm* and *chl27-t* mutants. Average SOLINA signal from four biological replicates was calculated on annotated genes grouped by their functions (tRNA, rRNA and protein-coding). Individual biological replicates are shown in Fig. S7A.

REFERENCES

1. Okada, Y. Sperm chromatin structure: Insights from in vitro to in situ experiments. *Curr. Opin. Cell Biol.* **75**, 102075 (2022).

2. Zaheri, B. & Morse, D. An overview of transcription in dinoflagellates. *Gene* **829**, 146505 (2022).

3. Laursen, S. P., Bowerman, S. & Luger, K. Archaea: The Final Frontier of Chromatin. *J. Mol. Biol.* **433**, 166791 (2021).

4. Lioy, V. S., Junier, I. & Boccard, F. Multiscale Dynamic Structuring of Bacterial Chromosomes. *Annu. Rev. Microbiol.* **75**, 541–561 (2021).

5. Sun, S., Rao, V. B. & Rossmann, M. G. Genome packaging in viruses. *Curr. Opin. Struct. Biol.* **20**, 114–120 (2010).

6. Powikrowska, M., Oetke, S., Jensen, P. E. & Krupinska, K. Dynamic composition, shaping and organization of plastid nucleoids. *Front. Plant Sci.* **5**, (2014).

7. Farge, G. & Falkenberg, M. Organization of DNA in Mammalian Mitochondria. *Int. J. Mol. Sci.* **20**, 2770 (2019).

8. Melonek, J., Oetke, S. & Krupinska, K. Multifunctionality of plastid nucleoids as revealed by proteome analyses. *Biochim. Biophys. Acta BBA - Proteins Proteomics* **1864**, 1016–1038 (2016).

9. Krupinska, K., Melonek, J. & Krause, K. New insights into plastid nucleoid structure and functionality. *Planta* **237**, 653–664 (2013).

10. Lindbeck, A. G. C., Rose, R. J., Lawrence, M. E. & Possingham, J. V. The role of chloroplast membranes in the location of chloroplast DNA during the greening ofPhaseolus vulgaris etioplasts. *Protoplasma* **139**, 92–99 (1987).

11. Sakai, A., Takano, H. & Kuroiwa, T. Organelle Nuclei in Higher Plants: Structure, Composition, Function, and Evolution. in *International Review of Cytology* vol. 238 59–118 (Academic Press, 2004).

12. Hansmann, P., Falk, H., Ronai, K. & Sitte, P. Structure, composition, and distribution of plastid nucleoids in Narcissus pseudonarcissus. *Planta* **164**, 459–472 (1985).
13. Sato, N., Nakayama, M. & Hase, T. The 70-kDa major DNA-compacting protein of the chloroplast nucleoid is sulfite reductase. *FEBS Lett.* **487**, 347–350 (2001).
14. Cannon, G. C., Ward, L. N., Case, C. I. & Heinhorst, S. The 68 kDa DNA compacting nucleoid protein from soybean chloroplasts inhibits DNA synthesis in vitro. *Plant Mol. Biol.* **39**, 835–845 (1999).
15. Briat, J. F., Gigot, C., Laulhere, J. P. & Mache, R. Visualization of a Spinach Plastid Transcriptionally Active DNA-Protein Complex in a Highly Condensed Structure. *Plant Physiol.* **69**, 1205–1211 (1982).
16. Lehniger, M.-K. *et al.* Global RNA association with the transcriptionally active chromosome of chloroplasts. *Plant Mol. Biol.* **95**, 303–311 (2017).
17. Lindbeck, A. G. C. & Rose, R. J. Is DNA Associated with Spinach Chloroplast Vesicles at Specific Sites? *J. Plant Physiol.* **129**, 425–434 (1987).
18. Lindbeck, A. G. C. & Rose, R. J. Thylakoid-bound chloroplast DNA from spinach is enriched for replication forks. *Biochem. Biophys. Res. Commun.* **172**, 204–210 (1990).
19. Nemoto, Y., Kawano, S., Nagata, T. & Kuroiwa, T. Studies on Plastid-Nuclei (Nucleoids) in Nicotiana tabacum L. IV. Association of Chloroplast-DNA with Proteins at Several Specific Sites in Isolated Chloroplast-Nuclei. *Plant Cell Physiol.* **32**, 131–141 (1991).
20. Vora, T., Hottes, A. K. & Tavazoie, S. Protein occupancy landscape of a bacterial genome. *Mol. Cell* **35**, 247–253 (2009).
21. Freddolino, P. L., Amemiya, H. M., Goss, T. J. & Tavazoie, S. Dynamic landscape of protein occupancy across the Escherichia coli chromosome. *PLOS Biol.* **19**, e3001306 (2021).

22. Palomar, V. M., Jaksich, S., Fujii, S., Kuciński, J. & Wierzbicki, A. T. High-resolution map of plastid-encoded RNA polymerase binding patterns demonstrates a major role of transcription in chloroplast gene expression. *Plant J.* **111**, 1139–1151 (2022).
23. Yagi, Y., Ishizaki, Y., Nakahira, Y., Tozawa, Y. & Shiina, T. Eukaryotic-type plastid nucleoid protein pTAC3 is essential for transcription by the bacterial-type plastid RNA polymerase. *Proc. Natl. Acad. Sci. U. S. A.* **109**, 7541–7546 (2012).
24. Majeran, W. *et al.* Nucleoid-Enriched Proteomes in Developing Plastids and Chloroplasts from Maize Leaves: A New Conceptual Framework for Nucleoid Functions. *Plant Physiol.* **158**, 156–189 (2012).
25. Pfalz, J., Liere, K., Kandlbinder, A., Dietz, K.-J. & Oelmüller, R. pTAC2, -6, and -12 Are Components of the Transcriptionally Active Plastid Chromosome That Are Required for Plastid Gene Expression. *Plant Cell* **18**, 176–197 (2006).
26. Melonek, J., Matros, A., Trösch, M., Mock, H.-P. & Krupinska, K. The Core of Chloroplast Nucleoids Contains Architectural SWIB Domain Proteins. *Plant Cell* **24**, 3060–3073 (2012).
27. Buenrostro, J. D., Giresi, P. G., Zaba, L. C., Chang, H. Y. & Greenleaf, W. J. Transposition of native chromatin for fast and sensitive epigenomic profiling of open chromatin, DNA-binding proteins and nucleosome position. *Nat. Methods* **10**, 1213–1218 (2013).
28. Liu, J. W. & Rose, R. J. The spinach chloroplast chromosome is bound to the thylakoid membrane in the region of the inverted repeat. *Biochem. Biophys. Res. Commun.* **184**, 993–1000 (1992).
29. Klasek, L., Inoue, K. & Theg, S. M. Chloroplast Chaperonin-Mediated Targeting of a Thylakoid Membrane Protein. *Plant Cell* **32**, 3884–3901 (2020).

30. Cline, K., Henry, R., Li, C. & Yuan, J. Multiple pathways for protein transport into or across the thylakoid membrane. *EMBO J.* **12**, 4105–4114 (1993).
31. Endow, J. K., Singhal, R., Fernandez, D. E. & Inoue, K. Chaperone-assisted Post-translational Transport of Plastidic Type I Signal Peptidase 1*. *J. Biol. Chem.* **290**, 28778–28791 (2015).
32. Schuler, M. A. & Zielinski, R. E. 3A - Preparation of Intact Chloroplasts from Pea. in *Methods in Plant Molecular Biology* (eds. Schuler, M. A. & Zielinski, R. E.) 39–47 (Academic Press, San Diego, 1989). doi:10.1016/B978-0-12-632340-5.50007-X.
33. Finster, S., Eggert, E., Zoschke, R., Weihe, A. & Schmitz-Linneweber, C. Light-dependent, plastome-wide association of the plastid-encoded RNA polymerase with chloroplast DNA. *Plant J. Cell Mol. Biol.* **76**, 849–860 (2013).
34. Zoschke, R. & Barkan, A. Genome-wide analysis of thylakoid-bound ribosomes in maize reveals principles of cotranslational targeting to the thylakoid membrane. *Proc. Natl. Acad. Sci.* **112**, E1678–E1687 (2015).
35. Pontier, D., Albrieux, C., Joyard, J., Lagrange, T. & Block, M. A. Knock-out of the magnesium protoporphyrin IX methyltransferase gene in Arabidopsis. Effects on chloroplast development and on chloroplast-to-nucleus signaling. *J. Biol. Chem.* **282**, 2297–2304 (2007).
36. Yao, Y. *et al.* Physiological, Cytological, and Transcriptomic Analysis of Magnesium Protoporphyrin IX Methyltransferase Mutant Reveal Complex Genetic Regulatory Network Linking Chlorophyll Synthesis and Chloroplast Development in Rice. *Plants Basel Switz.* **12**, 3785 (2023).
37. Bang, W. Y. *et al.* Role of Arabidopsis CHL27 Protein for Photosynthesis, Chloroplast Development and Gene Expression Profiling. *Plant Cell Physiol.* **49**, 1350–1363 (2008).

38. Chi, W., He, B., Mao, J., Jiang, J. & Zhang, L. Plastid sigma factors: Their individual functions and regulation in transcription. *Biochim. Biophys. Acta* **1847**, 770–778 (2015).
39. Ishizaki, Y. *et al.* A nuclear-encoded sigma factor, Arabidopsis SIG6, recognizes sigma-70 type chloroplast promoters and regulates early chloroplast development in cotyledons. *Plant J. Cell Mol. Biol.* **42**, 133–144 (2005).
40. Kanamaru, K. *et al.* An Arabidopsis sigma factor (SIG2)-dependent expression of plastid-encoded tRNAs in chloroplasts. *Plant Cell Physiol.* **42**, 1034–1043 (2001).
41. Fujii, S. *et al.* Impacts of phosphatidylglycerol on plastid gene expression and light induction of nuclear photosynthetic genes. *J. Exp. Bot.* **73**, 2952–2970 (2022).
42. Kobayashi, K. *et al.* Role of galactolipid biosynthesis in coordinated development of photosynthetic complexes and thylakoid membranes during chloroplast biogenesis in Arabidopsis. *Plant J. Cell Mol. Biol.* **73**, 250–261 (2013).
43. Greiner, S. *et al.* Chloroplast nucleoids are highly dynamic in ploidy, number, and structure during angiosperm leaf development. *Plant J.* **102**, 730–746 (2020).
44. Ruedas, R. *et al.* Three-Dimensional Envelope and Subunit Interactions of the Plastid-Encoded RNA Polymerase from Sinapis alba. *Int. J. Mol. Sci.* **23**, 9922 (2022).
45. Jeong, S. Y., Rose, A. & Meier, I. MFP1 is a thylakoid-associated, nucleoid-binding protein with a coiled-coil structure. *Nucleic Acids Res.* **31**, 5175–5185 (2003).
46. Sato, N. *et al.* Molecular characterization of the PEND protein, a novel bZIP protein present in the envelope membrane that is the site of nucleoid replication in developing plastids. *Plant Cell* **10**, 859–872 (1998).

47. Ingelsson, B. & Vener, A. V. Phosphoproteomics of Arabidopsis chloroplasts reveals involvement of the STN7 kinase in phosphorylation of nucleoid protein pTAC16. *FEBS Lett.* **586**, 1265–1271 (2012).

48. Weber, P. *et al.* TCP34, a nuclear-encoded response regulator-like TPR protein of higher plant chloroplasts. *J. Mol. Biol.* **357**, 535–549 (2006).

49. Woldringh, C. L. The role of co-transcriptional translation and protein translocation (transertion) in bacterial chromosome segregation. *Mol. Microbiol.* **45**, 17–29 (2002).

50. Irastortza-Olaziregi, M. & Amster-Choder, O. Coupled Transcription-Translation in Prokaryotes: An Old Couple With New Surprises. *Front. Microbiol.* **11**, (2021).

51. Snead, W. T. & Gladfelter, A. S. The Control Centers of Biomolecular Phase Separation: How Membrane Surfaces, PTMs, and Active Processes Regulate Condensation. *Mol. Cell* **76**, 295–305 (2019).

52. Woodson, J. D., Perez-Ruiz, J. M., Schmitz, R. J., Ecker, J. R. & Chory, J. Sigma factor-mediated plastid retrograde signals control nuclear gene expression. *Plant J. Cell Mol. Biol.* **73**, 1–13 (2013).

53. Nakatani, H. Y. & Barber, J. An improved method for isolating chloroplasts retaining their outer membranes. *Biochim. Biophys. Acta* **461**, 500–512 (1977).

54. Inskeep, W. P. & Bloom, P. R. Extinction Coefficients of Chlorophyll *a* and *b* in *N,N* -Dimethylformamide and 80% Acetone. *Plant Physiol.* **77**, 483–485 (1985).

55. Rowley, M. J., Böhmdorfer, G. & Wierzbicki, A. T. Analysis of long non-coding RNAs produced by a specialized RNA polymerase in Arabidopsis thaliana. *Methods* **63**, 160–169 (2013).

56. Porra, R. J., Thompson, W. A. & Kriedemann, P. E. Determination of accurate extinction coefficients and simultaneous equations for assaying chlorophylls a and b extracted with four different solvents: verification of the concentration of chlorophyll standards by atomic absorption spectroscopy. *Biochim. Biophys. Acta BBA - Bioenerg.* **975**, 384–394 (1989).
57. Kobayashi, K., Masuda, T., Takamiya, K. & Ohta, H. Membrane lipid alteration during phosphate starvation is regulated by phosphate signaling and auxin/cytokinin cross-talk. *Plant J.* **47**, 238–248 (2006).
58. Martin, M. Cutadapt removes adapter sequences from high-throughput sequencing reads. *EMBnet.journal* **17**, 10–12 (2011).
59. Langmead, B. & Salzberg, S. L. Fast gapped-read alignment with Bowtie 2. *Nat. Methods* **9**, 357–359 (2012).
60. Danecek, P. *et al.* Twelve years of SAMtools and BCFtools. *GigaScience* **10**, giab008 (2021).
61. Quinlan, A. R. & Hall, I. M. BEDTools: a flexible suite of utilities for comparing genomic features. *Bioinforma. Oxf. Engl.* **26**, 841–842 (2010).
62. Di, Y., Schafer, D. W., Cumbie, J. S. & Chang, J. H. The NBP Negative Binomial Model for Assessing Differential Gene Expression from RNA-Seq. *Stat. Appl. Genet. Mol. Biol.* **10**, (2011).

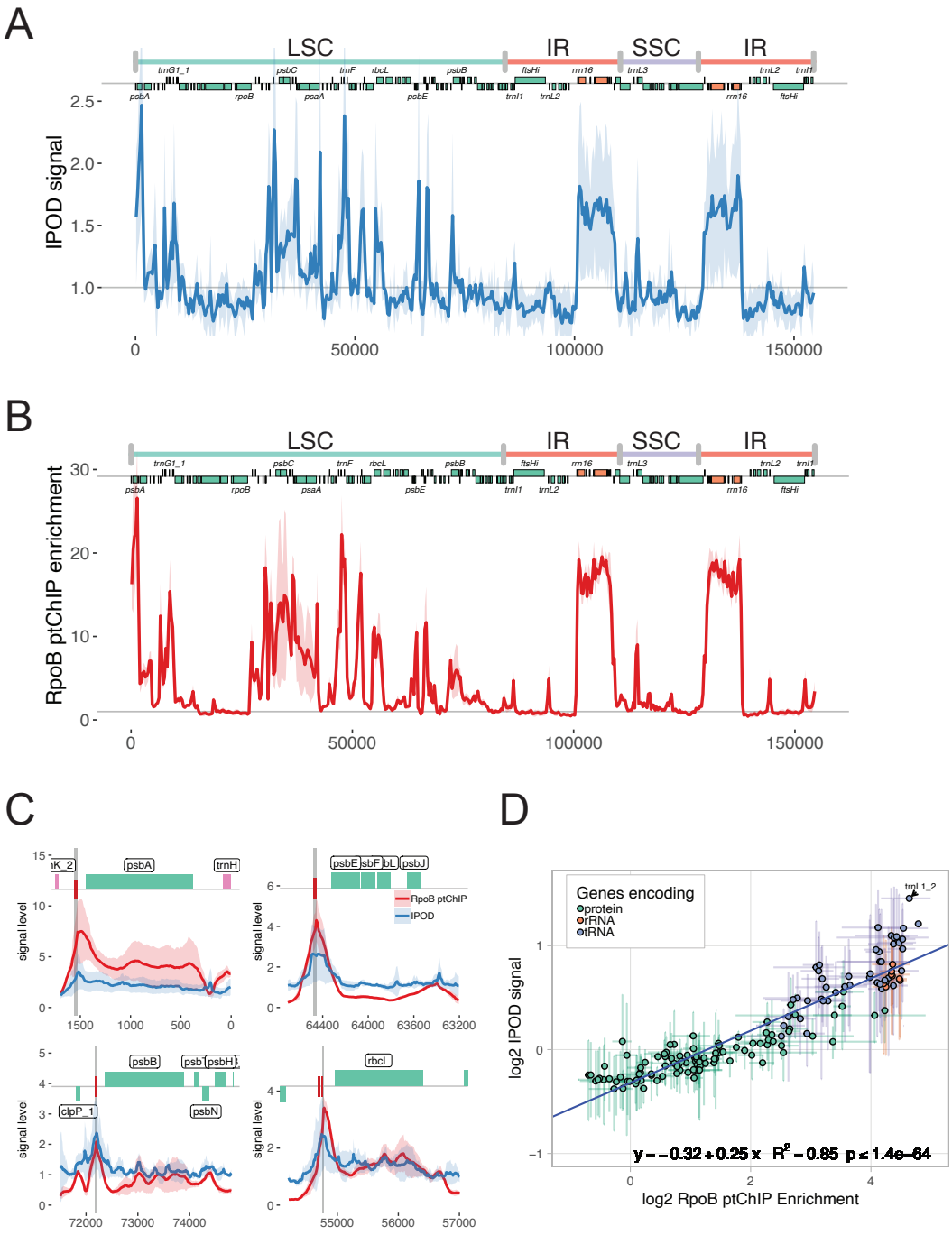
A
LSC
IR
SSC
IR
IPOD signal
2.5
2.0
1.5
1.0
0
50000
100000
150000
B
RpoB ptChIP enrichment
30
20
10
0
C
signal level
psbA
trnH
RpoB ptChIP
IPOD
psbB
clpP_1
psbN
rbcL
D
Genes encoding
protein
rRNA
tRNA
trnL1_2
log2 IPOD signal
log2 RpoB ptChIP Enrichment
y = −0.32 + 0.25 x R² = 0.85 p ≤ 1.4e−64

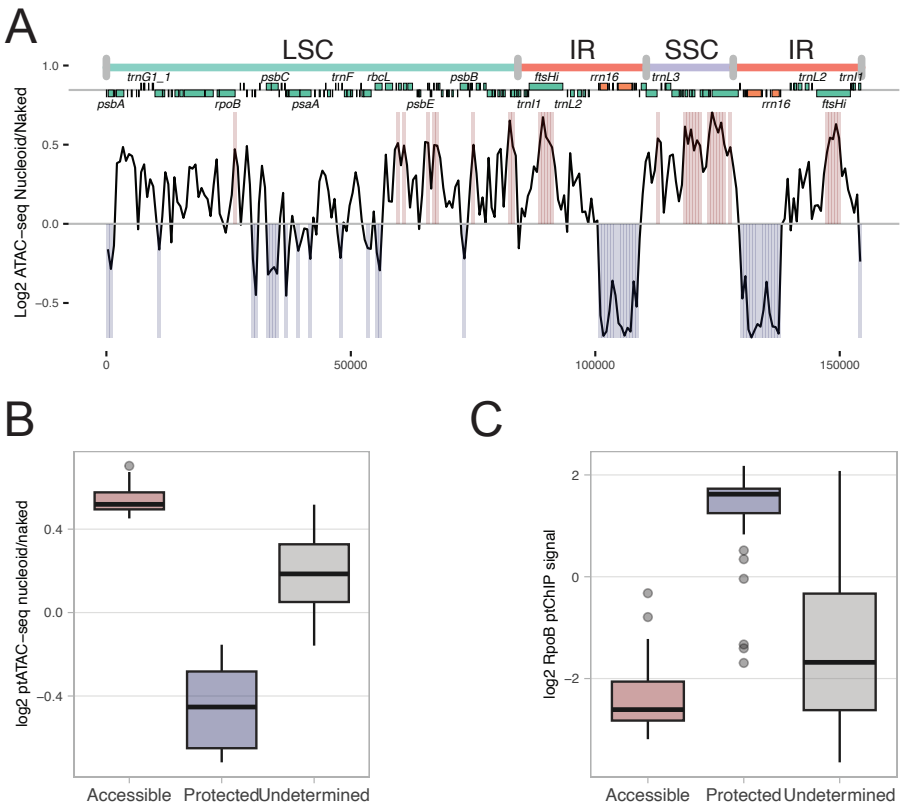
A
LSC
IR
SSC
IR
trnG1_1
psbC
trnF
rbcL
psbB
ftsHi
rrn16
trnL3
trnL2
trnI1
psbA
rpoB
psaA
psbE
trnI1
trnL2
rrn16
ftsHi
Log2 ATAC−seq Nucleoid/Naked
1.0
0.5
0.0
−0.5
0
50000
100000
150000
B
log2 ptATAC−seq nucleoid/naked
0.4
0.0
−0.4
Accessible
Protected
Undetermined
C
log2 RpoB ptChIP signal
2
0
−2
Accessible
Protected
Undetermined

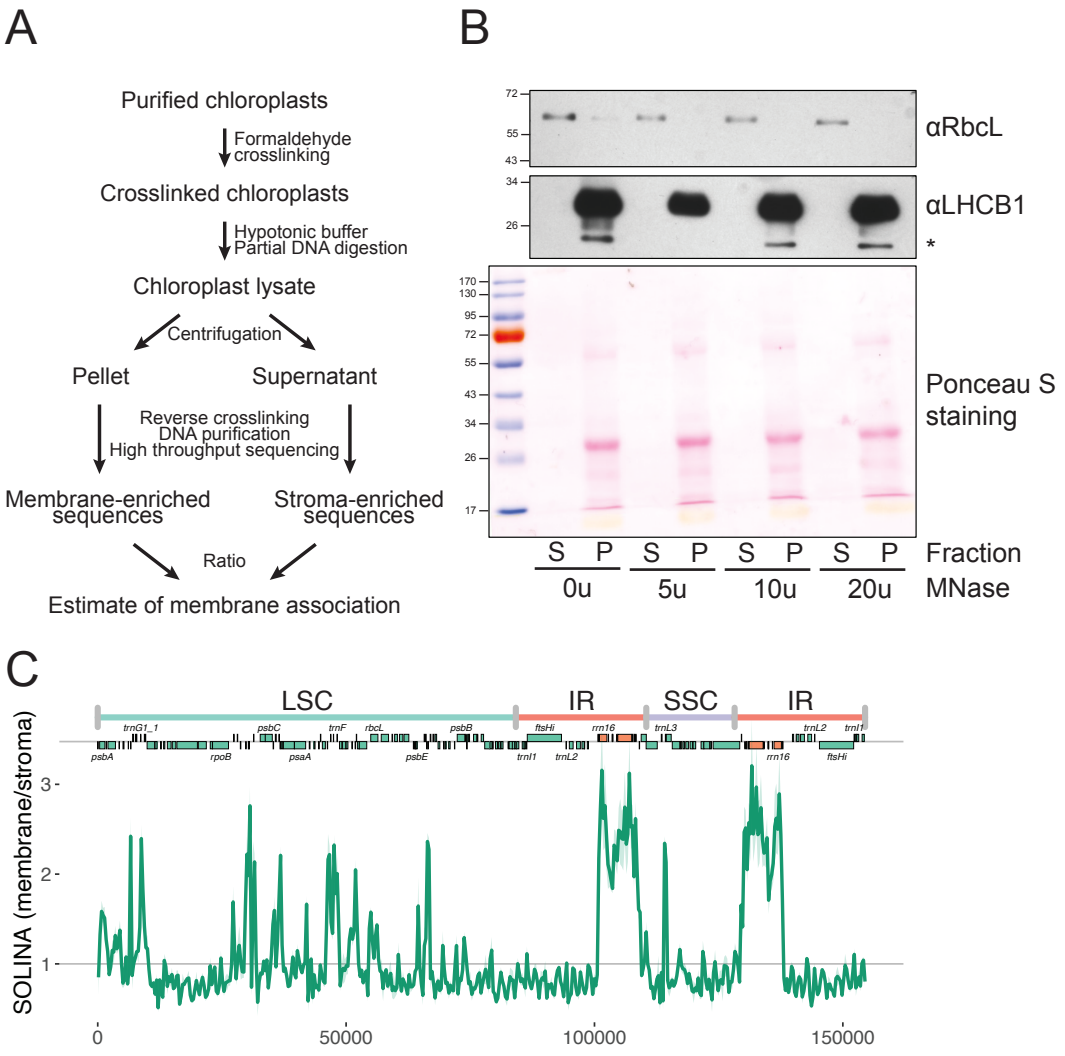
A
Purified chloroplasts
Formaldehyde crosslinking
Crosslinked chloroplasts
Hypotonic buffer Partial DNA digestion
Chloroplast lysate
Centrifugation
Pellet
Supernatant
Reverse crosslinking DNA purification High throughput sequencing
Membrane-enriched sequences
Stroma-enriched sequences
Ratio
Estimate of membrane association
B
αRbcL
αLHCB1
*
Ponceau S staining
S P S P S P S P
0u 5u 10u 20u
Fraction MNase
C
LSC
IR
SSC
IR
SOLINA (membrane/stroma)
0
50000
100000
150000

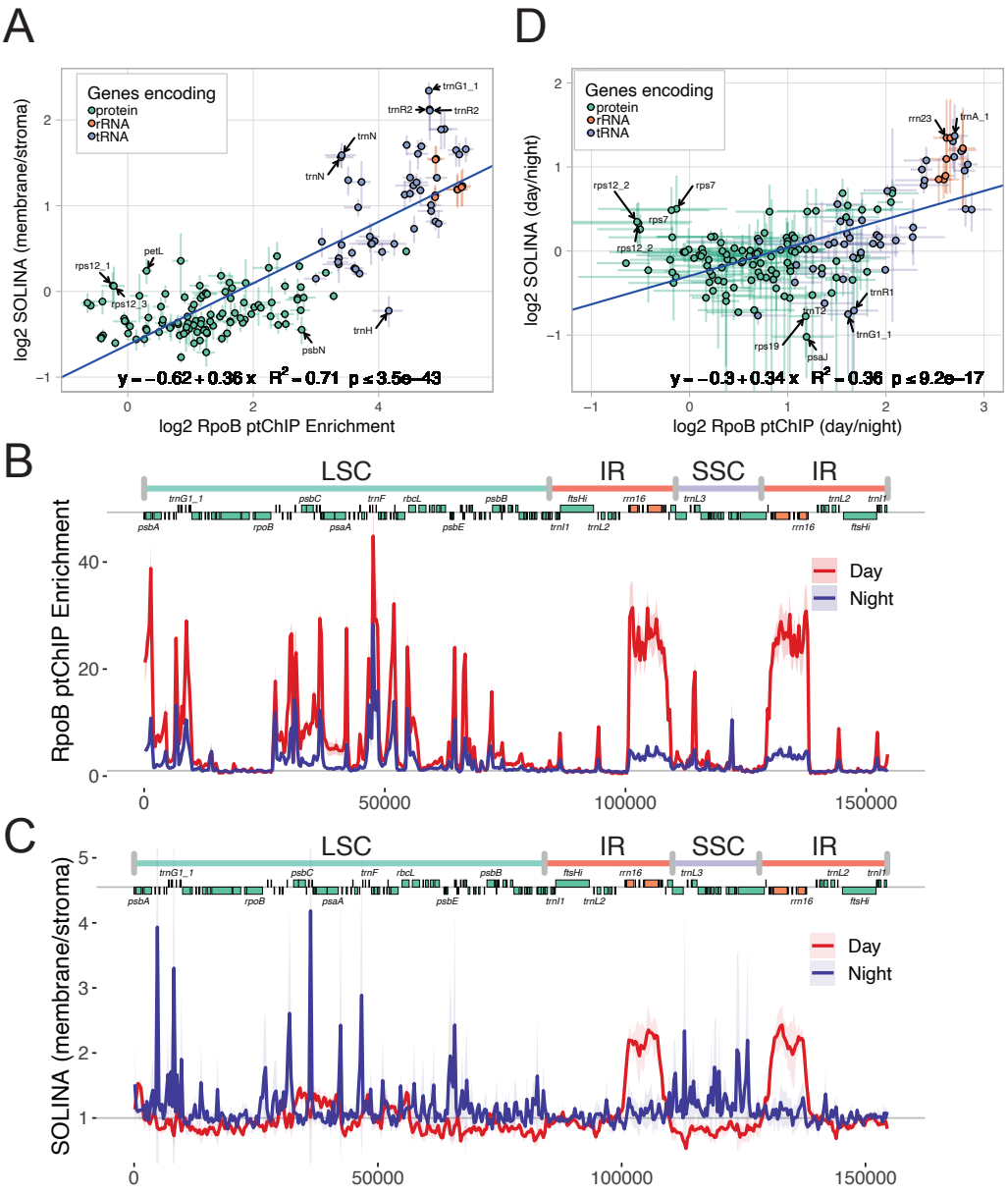
A
Genes encoding
protein
rRNA
tRNA
log2 SOLINA (membrane/stroma)
log2 RpoB ptChIP Enrichment
y = −0.62 + 0.36 x R² = 0.71 p ≤ 3.5e−43
trnG1_1
trnR2
trnN
petL
rps12_1
rps12_3
trnH
psbN
D
Genes encoding
protein
rRNA
tRNA
log2 SOLINA (day/night)
log2 RpoB ptChIP (day/night)
y = −0.3 + 0.34 x R² = 0.36 p ≤ 9.2e−17
rrn23
trnA_1
rps12_2
rps7
trnR1
trnT2
rps19
psaJ
trnG1_1
B
LSC
IR
SSC
IR
RpoB ptChIP Enrichment
Day
Night
C
SOLINA (membrane/stroma)
Day
Night

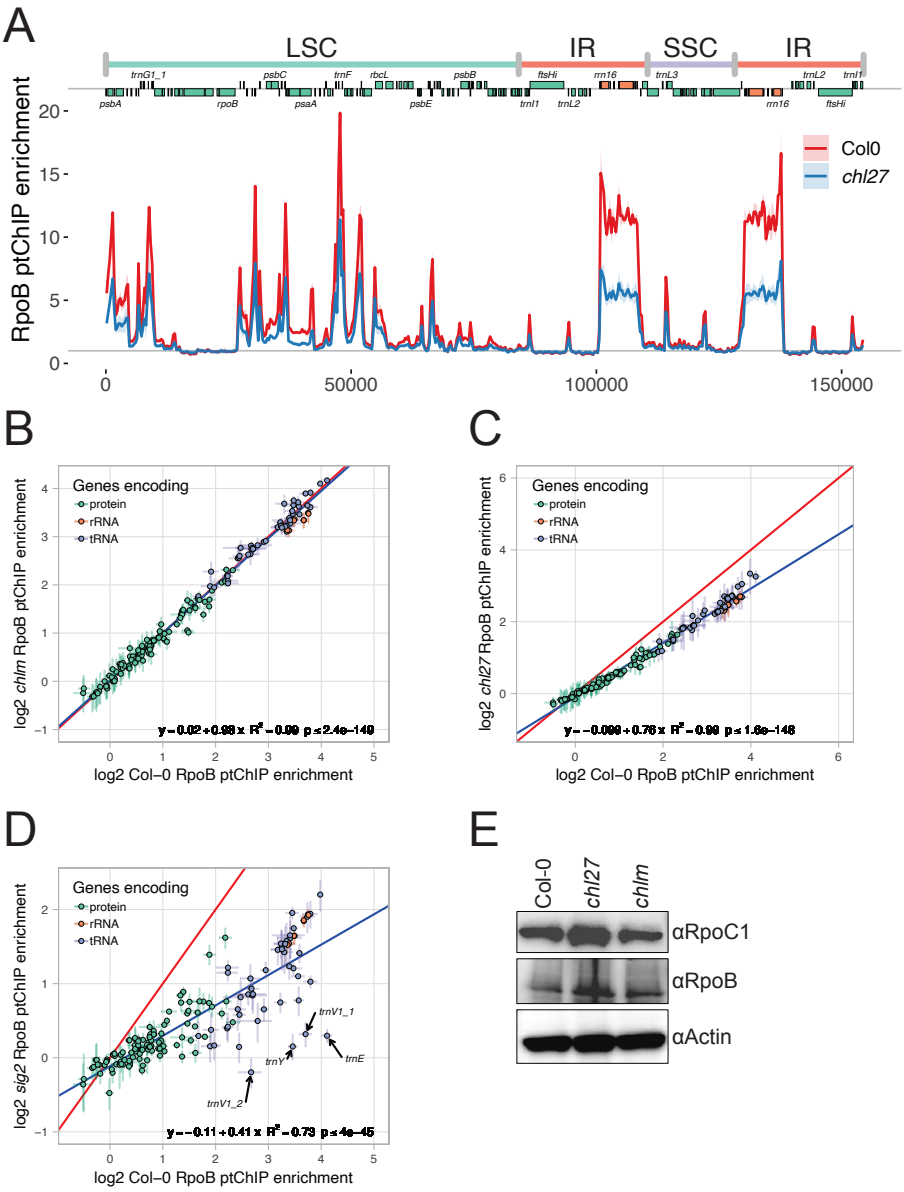
A
LSC
IR
SSC
IR
RpoB ptChIP enrichment
Col0
chl27
0
50000
100000
150000
B
Genes encoding
protein
rRNA
tRNA
log2 chlm RpoB ptChIP enrichment
log2 Col−0 RpoB ptChIP enrichment
C
log2 chl27 RpoB ptChIP enrichment
D
log2 sig2 RpoB ptChIP enrichment
trnV1_1
trnV
trnE
trnV1_2
E
Col-0
chl27
chlm
αRpoC1
αRpoB
αActin

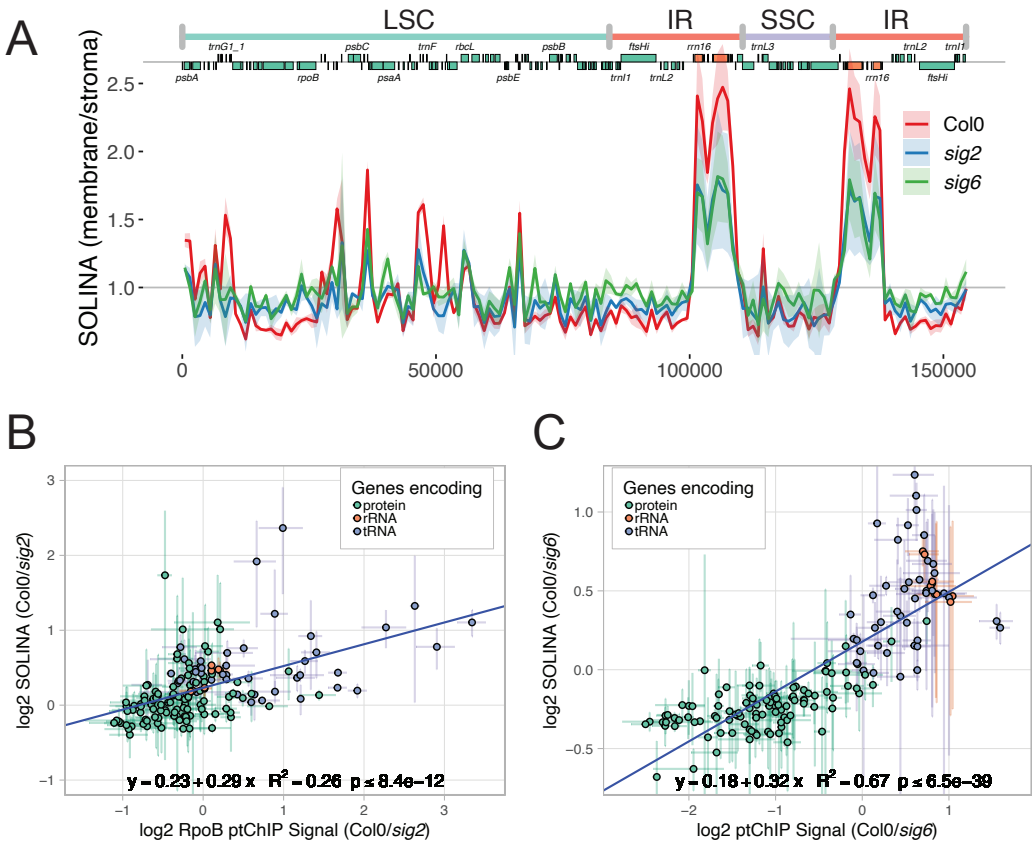
A
LSC
IR
SSC
IR
trnG1_1
psbC
trnF
rbcL
psbB
ftsHi
rrn16
trnL3
trnL2
trnI1
psbA
rpoB
psaA
psbE
trnI1
trnL2
rrn16
ftsHi
SOLINA (membrane/stroma)
2.5
2.0
1.5
1.0
0
50000
100000
150000
Col0
sig2
sig6
B
Genes encoding
protein
rRNA
tRNA
log2 SOLINA (Col0/sig2)
y = 0.23 + 0.29 x R2 = 0.26 p ≤ 8.4e−12
log2 RpoB ptChIP Signal (Col0/sig2)
C
Genes encoding
protein
rRNA
tRNA
log2 SOLINA (Col0/sig6)
y = 0.18 + 0.32 x R2 = 0.67 p ≤ 6.5e−39
log2 ptChIP Signal (Col0/sig6)

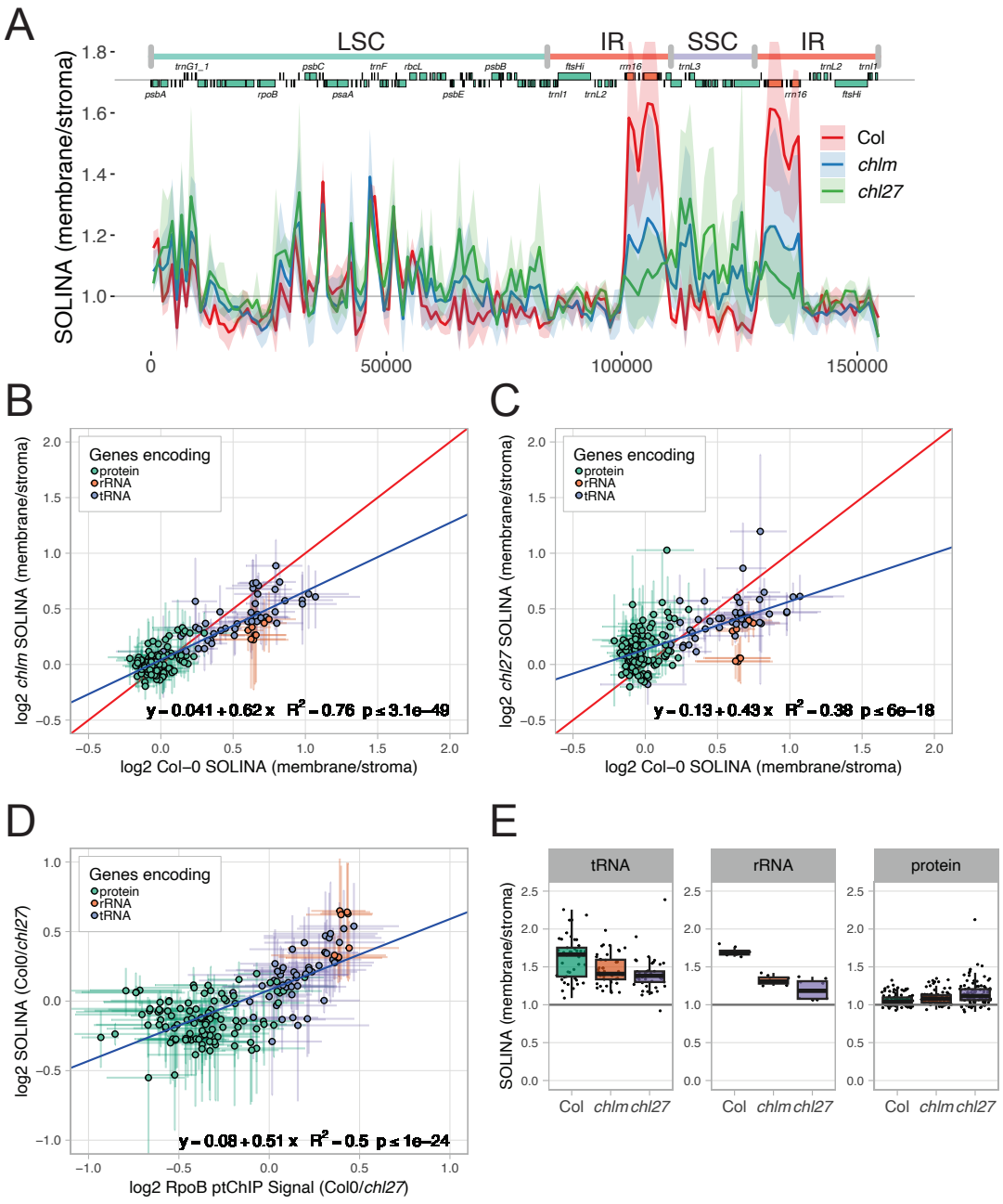
A
LSC
IR
SSC
IR
trnG1_1
psbC
trnF
rbcL
psbB
ftsHi
rrn16
trnL3
trnL2
trnI1
psbA
rpoB
psaA
psbE
trnI1
trnL2
rrn16
ftsHi
SOLINA (membrane/stroma)
1.8
1.6
1.4
1.2
1.0
0
50000
100000
150000
Col
chlm
chl27
B
log2 chlm SOLINA (membrane/stroma)
Genes encoding
protein
rRNA
tRNA
y = 0.041 + 0.62 x R² = 0.76 p ≤ 3.1e−49
log2 Col−0 SOLINA (membrane/stroma)
C
log2 chl27 SOLINA (membrane/stroma)
Genes encoding
protein
rRNA
tRNA
y = 0.13 + 0.43 x R² = 0.38 p ≤ 6e−18
log2 Col−0 SOLINA (membrane/stroma)
D
log2 SOLINA (Col0/chl27)
Genes encoding
protein
rRNA
tRNA
y = 0.08 + 0.51 x R² = 0.5 p ≤ 1e−24
log2 RpoB ptChIP Signal (Col0/chl27)
E
SOLINA (membrane/stroma)
tRNA
rRNA
protein
Col
chlm
chl27